

## Vertical distribution of microplastic along the main gate of Indonesian Throughflow pathways



Corry Yanti Manullang <sup>a,b,c</sup>, Mufti Petala Patria <sup>a,\*</sup>, Agus Haryono <sup>d</sup>, Sabiqah Tuan Anuar <sup>e,f</sup>, Muhammad Fadli <sup>b,c</sup>, Raden Dwi Susanto <sup>g,h</sup>, Zexun Wei <sup>i</sup>

<sup>a</sup> Department of Biology, Faculty of Mathematics and Natural Science, Universitas Indonesia, 16424 Depok, Indonesia

<sup>b</sup> Research Center for Deep Sea, National Research and Innovation Agency (BRIN), 97233 Ambon, Indonesia

<sup>c</sup> Center for Collaborative Research on Aquatic Ecosystem in Eastern Indonesia, 97233 Ambon, Indonesia

<sup>d</sup> Research Center for Chemistry, National Research and Innovation Agency (BRIN), 15314 Serpong, Indonesia

<sup>e</sup> Faculty of Science & Marine Environment, Universiti Malaysia Terengganu, 21030 Kuala Nerus, Terengganu, Malaysia

<sup>f</sup> Microplastic Research Interest Group, Universiti Malaysia Terengganu, 21030 Kuala Nerus, Terengganu, Malaysia

<sup>g</sup> Department of Atmospheric and Oceanic Science, University of Maryland, College Park, MD, USA

<sup>h</sup> Marine-Estuuarine and Environmental Sciences, University of Maryland, College Park, MD 20742, USA

<sup>i</sup> First Institute Oceanography, Ministry of Natural Resources, Qingdao, PR China

### ARTICLE INFO

#### Keywords:

Vertical distribution

Microplastic

Indonesian Throughflow

Makassar Strait

Lombok Strait

Alas Strait

### ABSTRACT

Even though Pacific – Indian Ocean exchange [Indonesian Throughflow (ITF)] has been measured for the last three decades, the measurements of microplastic in the region is very limited. This study was the initial investigation of the vertical distribution of microplastic in the deep-sea areas across the ITF Pathway. Niskin water samples were utilized to obtain the samples from a water column in a range of 5 to 2450 m. A total of 924 microplastic particles with an average abundance of  $1.062 \pm 0.646$  n/L were found in the water column. Our findings indicate that water temperature and water density are the most significant factors correlated to the microplastic concentration. This study will be the first report discussing the distribution of microplastics in the deep-sea water column that could be highly significant in determining the fate and transport of microplastic within Indonesian waters that exits into the Indian Ocean.

### 1. Introduction

Knowledge of the Pacific to Indian Ocean Exchange through the Indonesian seas is essential for understanding the role of the ocean in Earth's climate system. The Indonesian seas, with their complex geography and narrow passages, provide the only pathway for low-latitude Pacific water to flow into the Indian Ocean, a phenomenon known as the Indonesian Throughflow (ITF) (Susanto et al., 2016) (Supplementary material, Fig. S1). The ITF plays an integral role in global ocean thermohaline circulation, directly impacting mass, heat, and freshwater budgets of the Pacific and Indian Oceans. Additionally, it influences the El Niño Southern Oscillation (ENSO) and Asian-Australian monsoons (e.g., Bryden and Imawaki, 2001; De Deckker, 2016; Lee et al., 2002, 2019; Lee et al., 2015; Sprintall et al., 2009, 2014, 2019). The ITF is also crucial for downstream biogeochemistry (i.e., Ayers et al., 2014; Gorges et al., 2007), and the variability of ocean heat-content in the Indian

Ocean, particularly during the global warming (i.e., Lee et al., 2015; Makarim et al., 2019), as well as input and constraints for ocean-climate models (i.e., Metzger et al., 2010; Shinoda et al., 2012, 2016). The main inflow passage of the ITF originates in the western Pacific Ocean and enters the Indonesian seas through the Sulawesi sills, subsequently traversing the Sulawesi Sea and the Makassar Strait. From here, a portion of the water directly exits into the Indian Ocean via the Lombok and Alas Straits, while the majority flows to the Banda Sea and merges with the eastern ITF route before exiting into the Indian Ocean (Susanto et al., 2016). Along its path through Indonesian seas, the ITF experiences strong tidal mixing, which controls the water-mass stratification into the Indian Ocean (Pfield and Gordon, 1996; Hatayama, 2004; Hautala et al., 1996; Koch-Larrouy et al., 2007; Nagai and Hibiya, 2015; Nagai et al., 2021; Ray and Susanto, 2016, 2019; Susanto and Ray, 2022).

Fluxes of water, heat, and salt within the ITF, measured over the last three decades, have been identified as significantly influence global

\* Corresponding author.

E-mail address: [mpatria@sci.ui.ac.id](mailto:mpatria@sci.ui.ac.id) (M.P. Patria).

ocean thermohaline circulation (Susanto et al., 2016). Measurements of the ITF in the Makassar Strait have been conducted since the mid-1980s (Gordon et al., 1999, 2008; Susanto and Gordon, 2005; Susanto et al., 2012, 2000). However, there have been no accompanying measurements of ocean biogeochemistry that could provide insights into the impact of sub-seasonal, seasonal, and annual variability in the physical environment of the ITF on biogeochemical processes and fluxes, both within the ITF and downstream in the eastern Indian Ocean. Therefore, it is crucial to obtain biogeochemical measurements along the pathways of the ITF, particularly in the areas where the vertical distribution of pollutants remains unexplored and unknown.

Hence, in this research, we aim to fill this critical knowledge gap by presenting initial measurements of microplastic along the ITF Pathways. The issue of microplastic contamination throughout the ITF region should be investigated due to its potential impact to marine biota as well as human health. The ITF pathway indicates susceptibility to microplastic pollution, which is a result of the transportation of the ocean currents that traverse this area and anthropogenic activities in the surrounding area. Due to their negligible mass, microplastics exhibit high mobility and can be readily disseminated globally through oceanic currents. Meanwhile, anthropogenic activities such as maritime transportation, fisheries, and river runoff flowing into the sea have the potential to pollute this region. Despite being primarily found in coastal regions, multiple research studies have documented the presence of macroplastic and microplastic materials in nearby areas along the ITF pathway. A substantial amount of macroplastic in the Makassar Strait region has been reported (Isyirini et al., 2019). The study found that approximately 82–85 % of the total waste observed on the beach consisted of plastic and rubber waste. Research investigations have identified the presence of microplastics in various locations within the Makassar Strait, including seagrass habitats (Tahir et al., 2019a,b, 2020), salt ponds (Tahir et al., 2019a,b), estuary areas (Wicaksono et al., 2020), and coastal areas (Kama et al., 2021; Sawalman et al., 2021). The most up-to-date study reported that the concentration of microplastics >0.30–0.35 mm in the sea surface of Makassar Strait was very low (Yuan et al., 2023). Extensive research has been conducted on the presence of microplastics in benthos (Tahir et al., 2019a,b, 2020), milkfish obtained from brackish water pools (Amelinda et al., 2021), anchovies (Ningrum and Patria, 2022) and fishes (Rochman et al., 2015). Furthermore, studies have documented microplastics in coastal areas of the Bali Strait region (Suteja et al., 2021; Germanov et al., 2019). There have been no known reports of microplastics in the deep-sea area of ITF. There have been no known reports of microplastics in the water column of the deep-sea area of ITF. However, several investigations in oceanic and deep-sea regions indicate that these environments can serve as significant sinks for plastic waste (Woodall et al., 2014). This study represents the first investigation into microplastic concentrations in the deep sea along the ITF route. Additionally, this research contributes to understanding the fate of microplastics in the ocean. Several research investigations on microplastics conducted in the oceans have generally focused on the distribution of microplastics in the surface layer (Desforges et al., 2014; Enders et al., 2015; Kanhai et al., 2017; Lusher et al., 2014; Ross et al., 2021; Zhang et al., 2022). However, based on the estimates of the amount of plastic waste entering the ocean each year, several studies have raised questions about the quantity of waste found on the surface of the seawater (Eriksen et al., 2014). Recent research findings have indicated that plastic pollution in the ocean is not limited to the surface but also be present in deeper waters (Choy et al., 2019; Courten-Jones et al., 2017; Kanhai et al., 2018; Ross et al., 2021). Considering the knowledge gap regarding the imbalance between the volume of plastic input into the ocean and the documented amount of plastic on the ocean surface, the disclosure of microplastic concentrations from water columns can provide insight into the distribution and fate of microplastic in the ocean. Moreover, this study aligns with the assumption that the greater transfer of water masses from the Pacific Ocean to the Indian Ocean occurs at subsurface depths (Fan et al., 2018; Lu et al., 2023) and

that marine organisms are more densely populated within the water column than on the surface.

## 2. Materials and methods

### 2.1. Sample collection

Water samples were collected as part of the oceanographic cruise known as TRIUMPH (Throughflow Indonesian Seas, Upwelling and Mixing Physics). TRIUMPH is multidisciplinary and multinational collaborative research project involving scientists from the National Agency for Research and Innovation (BRIN) in Indonesia, the First Institute Oceanography (FIO) in China, and the University of Maryland in United States of America. The cruise took place aboard the R/V Baruna Jaya VIII, maintained by BRIN, from January 5 to April 1, 2021. The sampling process covered 11 stations, which were distributed across five distinct regions. These regions include the entrance of Makassar Strait consisting of three sites (R1, R2, R3); the Makassar Strait region representing by three stations (R4, R5, R6); the northern of Makassar Strait (R7); the Alas Strait (R8) and Lombok Strait regions were covered by three stations in total (R9, R10, R11) (Fig. 1). The water depth varied widely from 272 to 2512 m. Water column samples were collected from 8 to 10 depths at each station. However, at St. R8 and R11, the collection was conducted at only six layers due to the limited water depth (~200 m). The sampling depth level varied based on specific conditions, including the near-surface layer (~5 m); the maximum chlorophyll depth (Chl-Max) ranging from 30 to 65 m; the thermocline layer (upper, mid and bottom) between 50 and 400 m; the minimum dissolved oxygen depth (DO-Min) between 200 and 1500 m; and the near bottom depth from 200 to 2450 m. For water depths exceeding 1000 m, additional sampling was conducted at depths of 500 m, 750 m, 1000 m, 1500 m and 2000 m.

The collection of water samples from the water column and vertical profile of physical parameters was conducted using a carousel rosette water sampler consisting of 10 Niskin bottles set up with Sea-Bird SBE 911+ conductivity-temperature-depth (CTD) devices. The sample collection process involved obtaining the rosette bottle from the water column, starting from the lowest layer and ending at the sea surface (5 m). At each location, the CTD device was lowered closest to the bottom of the water. During the descent, the CTD instrument collects various physical properties of the water column, including temperature, salinity, and density. This data allowed the onboard operator to determine the maximum chlorophyll depth, thermocline layer, and minimum dissolved oxygen (DO) depth. Concurrent records of the physical-chemical parameters were carried out during the water sample collection to obtain precise and accurate values. A quantity ranging from 8 to 10 l was extracted from the rosette Niskin bottle and immediately subjected to filtration through a closed filtering system. The filtered water is collected in a bucket that facilitates precise measurement of the filtered volume. The filtering process was carefully executed to prevent potential air contamination during sample collection. The rosette Niskin bottle of water was attached to a natural rubber pipe. The water was subjected to filtration using a 20 µm nylon filter. The residual material accumulated on the filter was collected in a bucket to determine the volume of the filtrate. The material remaining on the filter was immediately transferred to a labelled glass bottle as a sample. Sample bottles were stored in a cool box before being transferred to the laboratory.

### 2.2. Laboratory analysis

In the laboratory, the sample volume went through a reduction process using a 37 µm steel filter. Subsequently, the sample was placed in an oven at a temperature of 40 °C for 24 h to evaporate the remaining water volume. Then, 3 ml of 30 % hydrogen peroxide (H<sub>2</sub>O<sub>2</sub>) was added to the sample and heated at 40 °C for 24 h. The use of 30 % H<sub>2</sub>O<sub>2</sub> as a method for degrading organic materials has been widely reported in

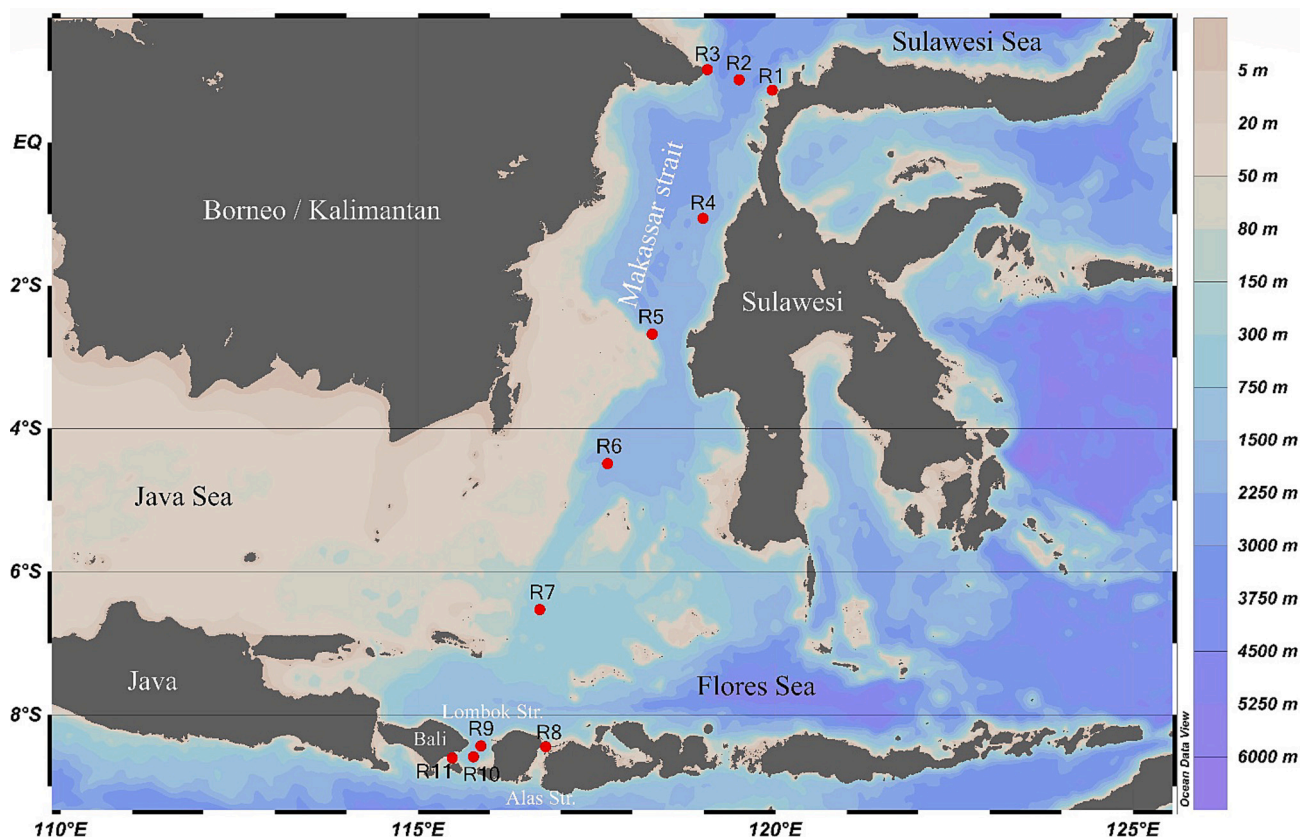


Fig. 1. Research station distribution of microplastic across the Indonesian Through Flow (ITF) pathway.

previous studies (Cordova et al., 2019, 2021; Suteja et al., 2021; Zhao et al., 2014). Next, the collected material was vacuum-filtered onto GF/C filter paper (47 mm, pore size: 0.47  $\mu\text{m}$ ) using a Buchner funnel and a vacuum flask. Each filter paper was then placed into a clean Petri dish and covered with an aluminium foil until the particles were quantified under a microscope. The samples were characterized using a Nikon SMZ645 stereo microscope with a magnification range of 40 $\times$ .

Previous research has suggested that various procedures for microscopic examinations to ensure accurate enumeration of microplastic particles. Microplastic particles exhibit distinct characteristics such as unnatural shapes and colors and a lack of fragility. Following previous research recommendations, fragility assessment was performed using a needle and tweezers. It has been suggested that microplastic particles maintain their structural integrity when subjected to pressure and displacement with needles and syringes (Horton et al., 2017; Suteja et al., 2021). Particle capturing was conducted using an Olympus SZX7 stereo microscope. Consistent with previous studies, particles were categorized into specific groups, including fragments, fibers, films, and pellets. Subsequently, the dimensions of the microplastic were assessed and recorded according to the following size categories: (i) 100–200  $\mu\text{m}$ ; (ii) 200–500  $\mu\text{m}$ ; (iii) 500–1000  $\mu\text{m}$  and (iv) 1000–2000  $\mu\text{m}$ .

The polymer test was conducted on a representative 20 % sample from each station using Horiba LabRAM HR Evolution Raman Spectrometer. Given the experimental protocol involving a blank method and subsequent degradation of organic compounds, it was determined that the 20 % proportion corresponds to the total number of samples. The prior study likewise allocated a proportion of 16–21 % of the whole sample for polymer identification testing (Cordova et al., 2020, 2021; Falahudin et al., 2020). The particles were analyzed directly on the filter surface using an optical microscope. The microscope was equipped with three objective lenses (10 $\times$ , 50 $\times$ , 100 $\times$ ). The particles were initially tested and detected using the 10 $\times$  objective lens before further analysis with the other two magnifications. The microscope focused the laser

beam on the selected particle surface. During the analysis, the lasers operated at approximately 10 to 50 % of their energy rating. A 785  $\mu\text{m}$  diode laser was used. Spectra were recorded in the spectral wave number range of 4000–600  $\text{cm}^{-1}$ . The obtained spectral characteristics of each sample were then compared to a standard polymer using the reference Micro-Raman Spectrometer. The polymer specimen for comparison was selected based on the highest percentage value in the Horiba micro-Raman spectrometer library. The mean match value generally exceeded 60 %.

### 2.3. Data analysis

This investigation reported the concentrations of microplastics in water column samples as particles or items per liter (n/L). Descriptive statistics were used to illustrate the number of plastic material pieces categorized by type and size. Additionally, the mean percentage of each plastic type was calculated from the overall plastic material collected. The statistical analysis was conducted using the Minitab software and R application. The Kolmogorov-Smirnov test was used to assess normality. Kruskal-Wallis tests were used to determine significant differences between stations. A one-way ANOVA test was conducted with a significance level of 0.05 to evaluate the significance of variations in microplastic concentration values across five different areas. A non-linear regression analysis was conducted using the Generalized Additive Model (GAM) in the R application to determine the physical parameters of the waters that impact the concentration of microplastics in the water column. The proposed GAM model applied the concentration of microplastics per layer at all stations as the response variable. Physical parameter data obtained from the CTD sensor, particularly salinity, temperature and density recorded during water column sampling, were used as the predictor variable. Ocean Data View 4 was utilized to generate contour graphs and maps (<http://odv.awi.de>).

The specific gravity of microplastic, the density of seawater, shape

and size of microplastic were used to calculate the settling velocity of microplastic (W). The W was calculated as Eq. (1) derived from [Francalanci et al. \(2021\)](#) and [Mancini et al. \(2023\)](#).

$$W = W^* (gRv)^{1/3} \quad (1)$$

where g represents the acceleration of gravity [ $\text{m/s}^2$ ]; R denotes the submerged relative density  $(\rho_{\text{MP}} - \rho) / \rho$  where  $\rho$  and  $\rho_{\text{MP}}$  denote the densities of seawater and microplastic, respectively; v signifies the fluid kinematic viscosity [ $\text{m}^2/\text{s}$ ] and  $W^*$  signifies the dimensionless settling velocity. The value of  $W^*$  can be determined using the following mathematical equation:

$$W^* = \frac{D_*^2}{C_1 + (0.75C_2D_*^3)^n} \quad (2)$$

$D_*$  is the dimensionless reference diameter defined as follows:

$$D_* = D_g \left( \frac{gR}{v^2} \right)^{1/2} \quad (3)$$

$D_g$  is the representative diameter that consider the shape defined as follows:

$$D_g = a(CSF)^{0.34} \left( \frac{b}{a} \right)^{0.5} \quad (4)$$

$C_1$  is a dimensionless coefficient dependent, defines as follows:

$$C_1 = 18E^{-0.38} \quad (5)$$

E is defined as follows:

$$E = a \left( \frac{a^2 + b^2 + c^2}{3} \right)^{1/2} \quad (6)$$

where a, b and c are the longest, the intermediate, and the shortest axis, respectively of the measured particles.

$C_2$  and  $n$  are two dimensionless coefficients dependent on the Corey Shape Factor (CSF), defined as follows:

$$C_2 = 0.3708(CSF)^{-0.1602} \quad (7)$$

$$n = 0.4942(CSF)^{-0.059} \quad (8)$$

where CSF is a dimensionless shape factor representing the relative flatness of the particle, defined as follows:

$$CSF = \frac{c}{\sqrt{ab}} \quad (9)$$

#### 2.4. Contamination prevention

Several precautions were taken to prevent contamination during the sampling process: (i) all research equipment used in the study was cleaned with distilled water and rinsed three times; (ii) the sample bottles were heated at 200 °C for 24 h to ensure there was no plastic residue left in them; at this temperature, it is estimated that all plastic had melted; (iii) the empty bottle was kept open during the process of transferring the sample from the rosette bottle to the sample bottle, and (iv) gloves (nitrile) were worn to minimize contamination. To avoid contamination during laboratory analytical procedures, numerous controls were implemented. Sample processing was conducted in a separate laboratory from other activities to prevent air contamination. The analysis chamber had air vents closed to reduce outdoor air intake. To minimize air contamination, the destruction process was conducted in a fume container ([Van Cauwenbergh et al., 2013](#)). Additionally, samples were always covered to minimize air exposure. The research apparatus used in the study was carefully cleaned with distilled water and rinsed three times. Steel filters, Petri dishes, and beaker glasses used to filter

the solution were heated for 24 h at a temperature of 200 °C to ensure no plastic filaments were left in the gaps. All study materials were filtered through a sieve with a mesh size of 37 µm to prevent contamination from the used chemical solution. During the analysis, one sterile filter paper was set in the working area as a control sample ([Cordova et al., 2021](#)).

### 3. Results

#### 3.1. Overview research findings

This research addressed a comprehensive analysis of 92 water samples obtained from the deep-sea seawater column along the ITF pathway, from the Makassar Strait to the Lombok Strait. A total of 924 particles were isolated from 872 L of water samples extracted from depths ranging from 5 m to 2450 m. The microplastics discovered in this research were predominantly fibers (91.3 %) and fragments (7.4 %) ([Fig. 2](#)). The results indicated that a significant proportion of the particles, precisely 39 %, consisted of large microplastics with a size ranging from 1000 to 2000 µm, followed by a size range of 500–1000 µm, which accounted for 25 % of the particles. Additionally, particles with a size range of 200–500 µm and 100–200 µm accounted for 23 % and 12 % of the total particles, respectively, as illustrated in [Fig. 2](#). A micro-RAMAN spectrometer analyzed 20 % of the isolated particles from each station. The Raman spectra analysis revealed that the isolated particles matched the reference spectra, which included a total of 10 types of polymers: Polypropylene (PP), Polypropylene imine (PPI), Polyethylene-co-vinyl acetate (EVA), Polyethylene imines (PEI), Polyvinyl butyral (PVB), Polyvinyl acetate (PVA), Polymethyl vinyl ether-co-maleic acid (PVEMA), Polyurethane foam (PUR), Polyester (PEST) and Polyacrylic acid/Carboxy vinyl polymer (PAA) ([Fig. 3](#)). Polymethyl vinyl ether-co-maleic acid was the most prevalent polymer type, accounting for 43 % of the total, while polyester constituted 22 %, Polypropylene 8 %, Polypropylene imine 8 % and Polyethylene imine 5 %.

No particles were detected in the blanks, indicating no air contamination or issues during laboratory analysis. The rosette bottle used to collect the water sample was made of polyvinyl chloride-based plastic, but this type of polymer was not detected in this study. Furthermore, the polymer materials used in the water filtration procedure on the boat (natural rubber hose, nylon filter) were not discovered in the samples of this study.

#### 3.2. The abundance of microplastics along the ITF pathway

Particles were detected at all observation stations, including those in waters exceeding 2000 m. However, particles were not evenly distributed across all depth layers. The mean concentration of microplastics detected in the water samples was  $1.062 \pm 0.646$  (0 to 3.4) n/L, with most concentrations falling within the range of 0 and 2.2 n/L. Nevertheless, the analysis revealed elevated concentration levels at various stations, particularly at Station R8 in the Alas Strait region, where concentrations were recorded as 2.7 n/L at a depth of 5 m and 3.4 n/L at 100 m. Similarly, St. R7 in the Makassar Strait area exhibited a concentration value of 3.2 n/L at a depth of 400 m. Additionally, St. R11 demonstrated a concentration value of 2.667 n/L at a depth of 5 m.

The mean concentration of microplastics per sampling location ranged from 0.802 to 1.528 n/L ([Fig. 4](#)). Station R8 in the Alas Strait had the highest average concentration, while St. R9 in the Lombok Strait had the lowest average concentration. The microplastic concentration in the 11 stations did not follow a normal distribution ( $p > 0.005$ ). The Kruskal-Wallis test was used to determine the significance of microplastic concentration among locations. The results of this Kruskal-Wallis test showed no statistically significant difference ( $p$ -value = 0.892) among the 11 locations.

The microplastic concentration across five distinct regions was varied. However, the statistical analysis revealed that there was no statistically significant variation in the average value of microplastic content

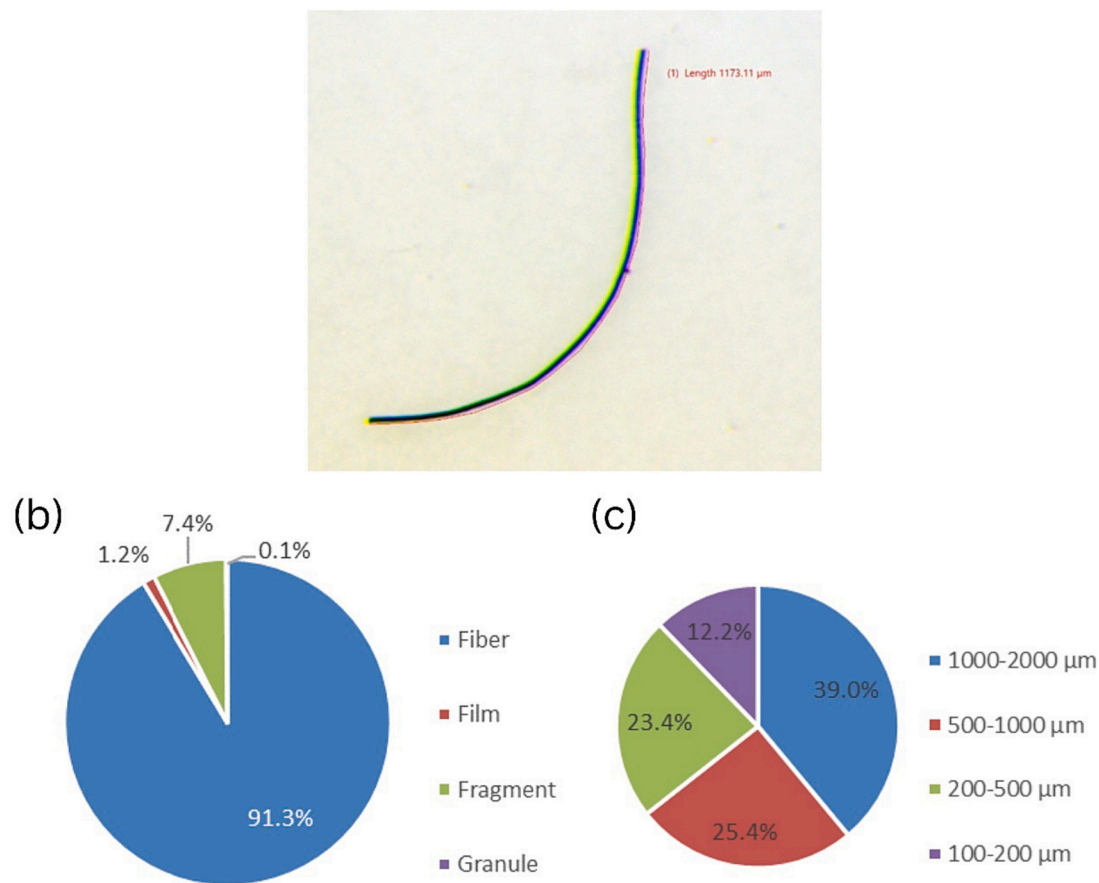


**Fig. 2.** Characteristic of microplastic found in the water column of ITF pathway. (a) The picture of fiber particles found in the ITF pathway. (b) The majority of the microplastics discovered in this study were fibers (91.3 %) and fragments (7.3 %). (c) The percentage of microplastic size found in the ITF pathway were 39 % of the particles consisted of microplastics measuring between 1000 and 2000  $\mu\text{m}$  in size. This was followed by a particle size range of 500–1000  $\mu\text{m}$ , which accounted for 25 % of the total particles. Particles with a size range of 200–500  $\mu\text{m}$  and 100–200  $\mu\text{m}$  accounted for 23 % and 12 % of the total particles.

among the five zones ( $p = 0.671$ ). The average concentration of microplastics in the area of the ITF entrance (R1, R2, R3) was  $1.093 \pm 0.398 \text{ n/L}$ . The mean microplastic concentration exhibited a reduction in the Makassar Strait (R4, R5, R6) to  $0.974 \pm 0.546 \text{ n/L}$ . In the southern region of the Makassar Strait (R7), the average concentration of microplastics subsequently elevated to  $1.113 \pm 0.854 \text{ n/L}$ . Significant increases in microplastic concentrations were observed in the Alas Strait (R8) with a range of  $1.528 \pm 1.281 \text{ n/L}$ . However, it was noted that the microplastic concentration decreased towards the Lombok Strait region (R9, R10, and R11), where it was quantified for  $0.987 \pm 0.705 \text{ n/L}$ . Based on statistical analysis, the average value of microplastic content did not exhibit any significant variation across the five oceanographic zones ( $p = 0.671$ ).

The north-south section of the microplastic concentration along the ITF pathway was described in the Fig. 5. The concentrations of microplastics (1–1.25 n/L) are found in layers shallower than 250 m and depth 500 to 1000 m. In the 500 m depth, a microplastic concentration of 0.5 n/L was detected. The basin areas seem susceptible to trapping microplastics.

The map illustrating the abundance of microplastics at several depths (5 m, 100 m, 200 m, 300 m, 500 m, and 1000 m) in the ITF gateway is presented in Fig. 6. At a depth of 5 m and 100 m, a significant concentration of microplastics was observed near the Alas Strait and Lombok Strait. The abundance of microplastics was also notable at a depth of 100 m in the Makassar Strait (near R6). Furthermore, elevated concentration of microplastics was observed near the entrance of Makassar Strait at depths of 200 m and 300 m. In the 500 m depth range, microplastic abundance was prominent at the entrance of Makassar

Strait, Alas Strait, and Lombok Strait. At a depth of 1000 m, microplastics were found to be abundant near the Makassar Strait.

### 3.3. Impact of environmental variables to the microplastic vertical distribution in the ITF pathway

The in-situ measurement of seawater's physical characteristics (temperature, salinity, and density) collected by CTD with plot microplastic abundance is described in Fig. 7. The temperature ranged from 3 to 29 °C. The salinity ranged between 31 and 34 psu, with lower values observed on the surface. The density ( $\sigma_t$ ) ranged between 19 and 27 kg/m<sup>3</sup>. The thermocline layer, located between 50 and 400 m deep, experiences significant temperature and density changes. The stations R4, R6, R8, R9, and R11 have the highest concentration of microplastics which were found within the density range ( $\sigma_t$ ) of 21–23 kg/m<sup>3</sup>. These stations also experience temperatures ranging from 25 to 28.50 °C and salinity levels between 33 and 34 psu. On the other hand, the stations R1, R2, R3, R7, and R10 exhibit the utmost concentrations of microplastics, which are observed within a density range ( $\sigma_t$ ) of 26–28 kg/m<sup>3</sup>, a temperature range of 3–10 °C, and a salinity range of 34–35 psu as depicted in Fig. 7.

A correlation analysis was conducted to investigate the relationship between the environmental physical parameters and the abundance of microplastics in the water column. The Spearman Rank correlation test was performed for this analysis, using the abundance of microplastics in the water column as the dependent variable and the physical parameters of the waters (temperature, salinity, and density) as the independent variables. Overall, the data demonstrated no significant statistical

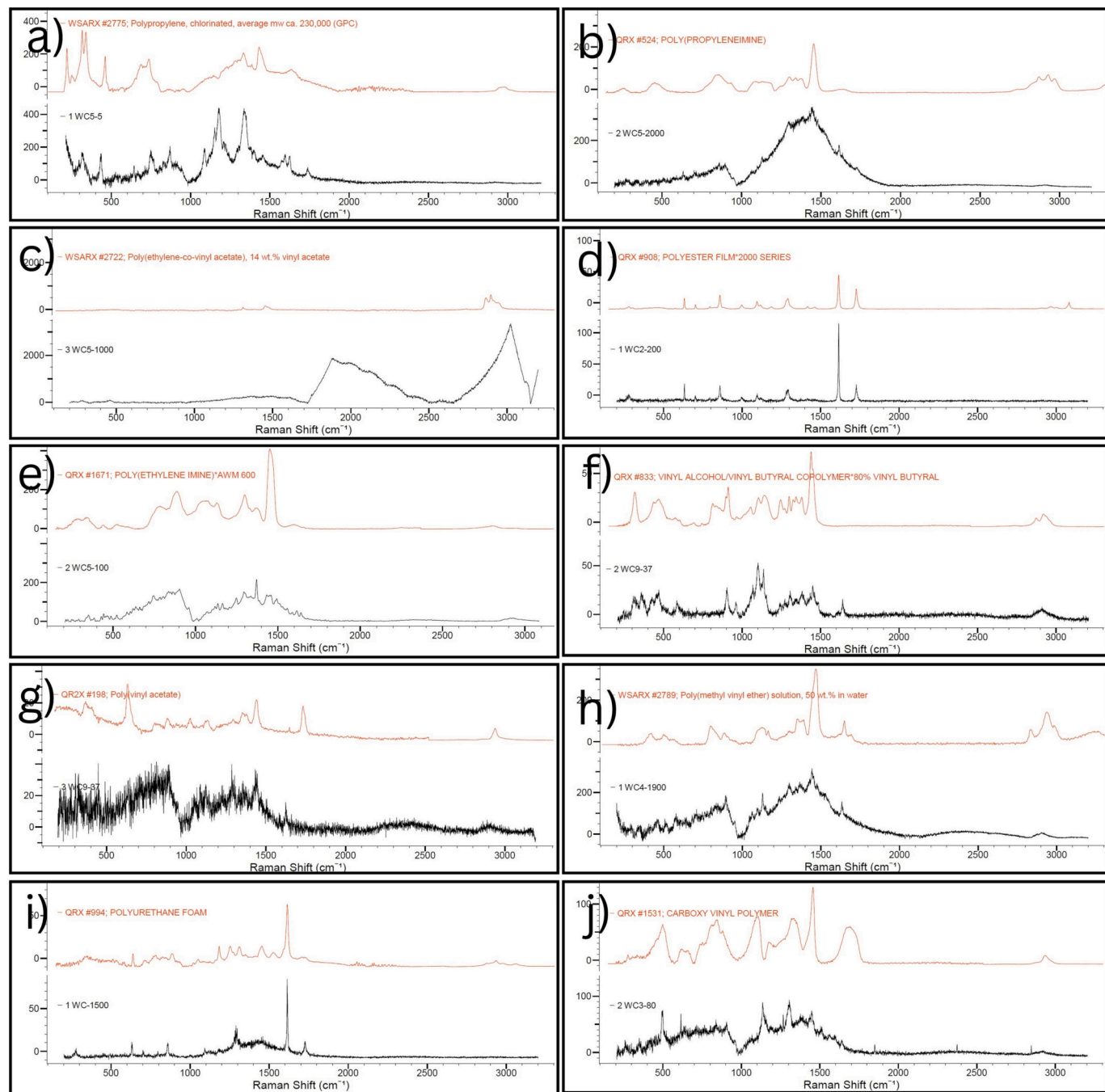


**Fig. 3.** Spectra of polymer across the ITF pathway (a) PP, (b) PPI, (c) EVA, (d) PEST, (e) PEI, (f) PVB, (g) PVA, (h) PVEMA, (i) PUR and (j) PAA. The red spectrum at the top of each quadrant represents the reference polymer in the RAMAN references. All black lines represent the spectra of particles recorded in this study.

correlation between the abundance of microplastics and the physical characteristics of the water ( $p$ -value  $> 0.05$ ;  $r < 0.25$ ).

Furthermore, a non-linear regression analysis using the Generalized Additive Model (GAM) was performed to identify the significant physical factors in the water that affect microplastic concentrations in the water column. In the GAM model, the concentration of microplastics per layer at all stations served as the response variable, while the water's physical parameter data acquired from the CTD sensor during water column sampling, including temperature, salinity, and density, were used as predictor variables. The GAM non-linear regression analysis yielded an R-sq value of 0.052 and explained 8.28 % of the deviance with the following formula:

$$\text{MPs} \sim s(\text{Salinity}) + s(\text{Temperature}) + s(\text{Density})$$

The study examined three predictor variables and found that water density and water temperature had a significant impact on the abundance of microplastics in the seawater column in the ITF waters of Indonesia, as seen in [Table 1](#). This result indicating that salinity, temperature and density partially have no effect to the microplastic concentration in the water column, whereas water density and water temperature affect the concentration value of the microplastic in the water column simultaneously.

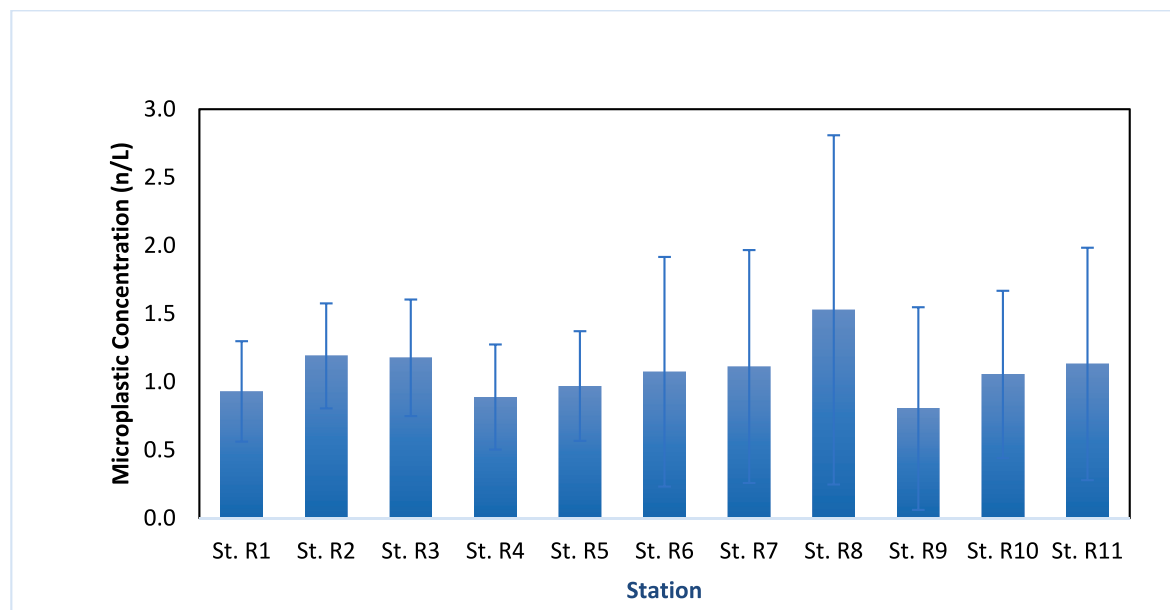


**Fig. 4.** The average concentration of microplastics at 11 stations along the ITF pathway. Station R8 in the Lombok Strait contained the greatest average concentration. Station R9 in the Lombok Strait enrolled the lowest average concentration. There is no statistically significant difference between the 11 locations.

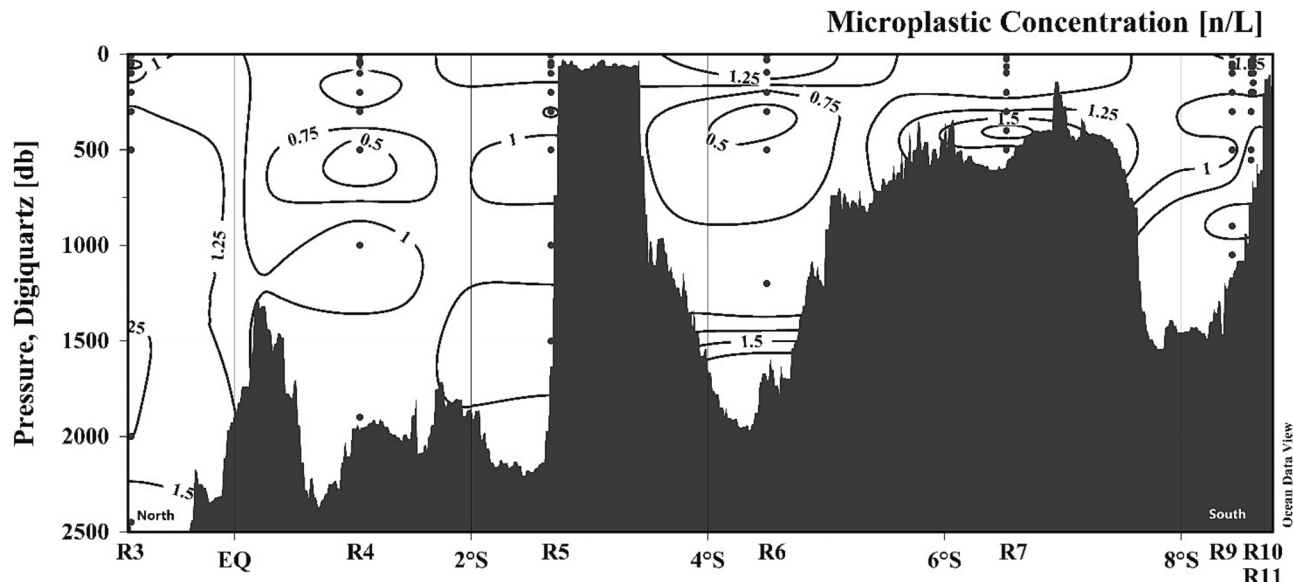


**Fig. 5.** North-south section of microplastic concentration along the main gate of ITF Pathways.

#### 3.4. Microplastic settling velocity

The settling velocity ( $W$ ) for each type of microplastic in this study was calculated following Eq. (1). We assumed all microplastic particles had the same CSF value in this study because fiber was the most commonly found type, accounting for 91 % of particles. The settling velocity range of microplastics in the ITF water column has been documented to be ranged between 0.0004 and 0.0068 m/s. The  $W$  for PEI, PPI, PAA, PVB, EVA, PP, PUR, PVA, PMVEMA, PEST were 0.0004 m/s, 0.0006 to 0.0007 m/s, 0.0008 m/s, 0.0014 m/s, 0.0014 m/s, 0.0019 m/s, 0.0029 m/s, 0.0031 m/s, 0.0063 to 0.0067 m/s and 0.0065 to 0.0068 m/s, respectively. The settling velocity for each polymer found is presented in the Supplementary material, Table S1.

#### 4. Discussion

Microplastics have been extensively documented across various global regions, including remote and pristine areas far from human influences. This study contributes to our understanding of the vertical distribution of microplastics in the deep-sea region by identifying microplastics at all stations along the ITF pathway. The ITF, located in Indonesian waters, is a part of the global inter-oceanic current cycle that circulates water masses from the Pacific Ocean to the Indian Ocean. Indonesia's strategic location at the convergence of these two major oceans leads to complex current dynamics that significantly impact the biological conditions of its waters. Consequently, Indonesian waters, which are traversed by these ocean currents, exhibit a high level of species diversity. However, it is expected that these currents also transport plastic waste, including microplastics, from other regions due

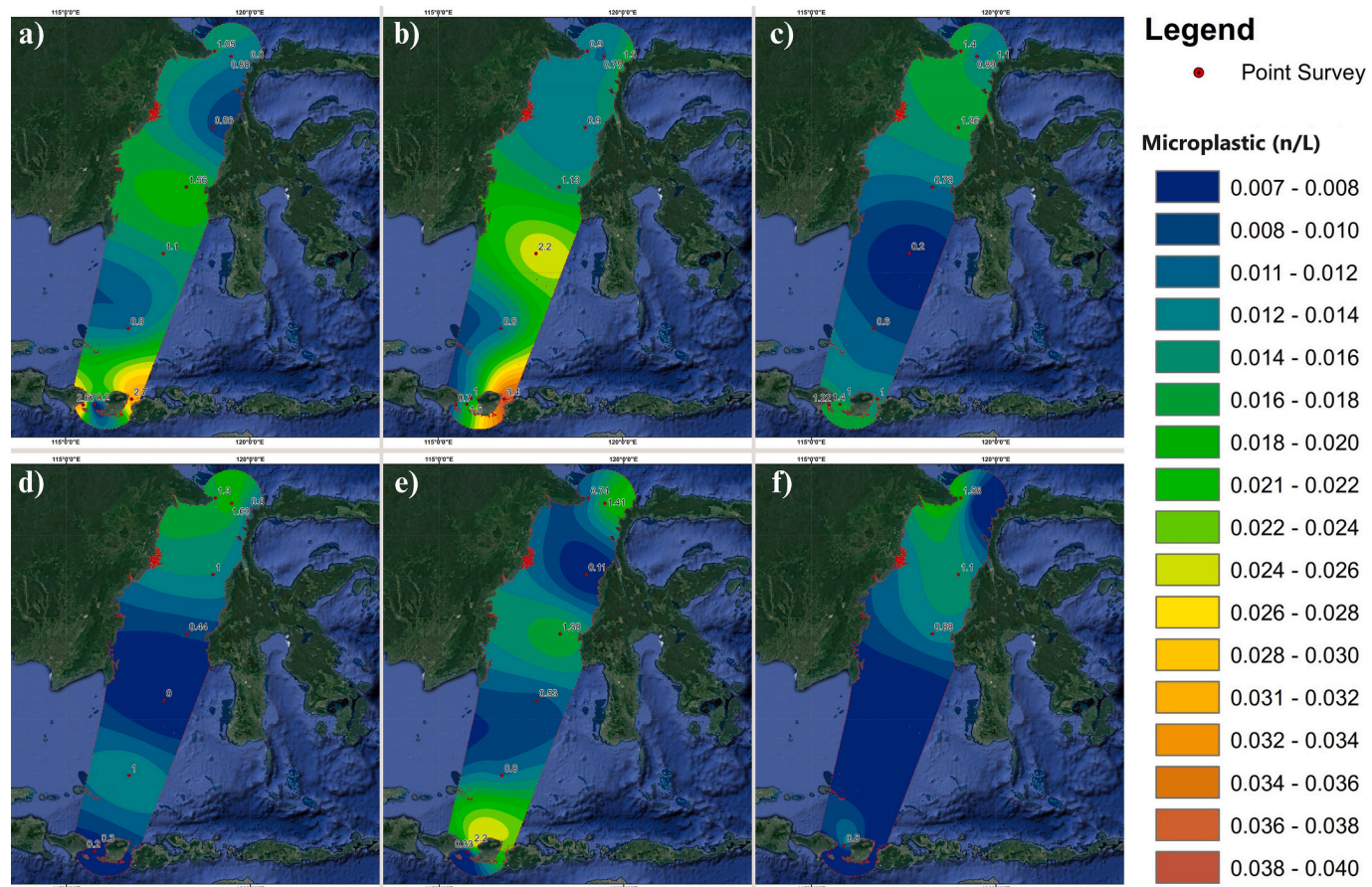


**Fig. 6.** Microplastic abundance at (a) 5 m, (b) 100 m, (c) 200 m, (d) 300 m, (e) 500 m and (f) 1000 m in the main gate of ITF. At depth 5 m and 100 m, the microplastic was high near the Alas strait and Lombok Strait. At depth 200 m and 300 m the microplastic abundance were higher in the entrance of Makassar Strait (R1, R2, R3). In the 500 m depth range, microplastic abundance was prominent at the entrance of Makassar Strait, Alas Strait, and Lombok Strait.

to the ease with which microplastics can be carried by ocean currents (Wang et al., 2020). Local activities, such as shipping and mainland inputs, can also contribute to contamination in this area. The presence of microplastics has raised concerns about their potential to disrupt various organisms' ecosystems. Multiple studies have indicated that these contaminants can be ingested by organisms, including zooplankton, small fish, and filter-feeding marine animals (filter-feeding megafauna). Numerous laboratory studies have demonstrated that microplastic pollution in marine organisms can lead to disruptions in photosynthetic activity (Bhattacharya et al., 2010), reduced appetite for zooplankton (Cole et al., 2013), decreased fecundity in zooplankton (Lee et al., 2013), lower body weight in lugworms (Besseling et al., 2013), the presence of an inflammatory immune response in clams (Von Moos et al., 2012), and decreased sperm diameter and speed in oysters (Sussarellu et al., 2016). Despite the microplastic quantities identified in this study being significantly lower than those examined in the laboratory tests, which ranged from 42,000 to 1,000,000 n/L, the detection of microplastics in this investigation raises concerns about the high biodiversity of the ITF area.

The microplastic fiber types found along the route from the Makassar Strait to the Lombok Strait as identified in this study are consistent with those found in other marine environments worldwide, both above and below water's surface (Choy et al., 2019; Kanhai et al., 2017; Lusher et al., 2015; Obbard et al., 2014; Peng et al., 2018). Many of the microplastic fibers discovered in the water are believed to originate from laundry wastewater. Experiments conducted by Napper and Thompson (2016) estimated that the average laundering of acrylic fabrics released over 700,000 fibers during a single wash. Furthermore, Vassilenko et al. (2019) revealed that 9777 to 4,315,371 microfibers were lost in every 1 kg of textile washed.

Polymer analysis is crucial in microplastic studies as it helps confirm the types of particles obtained. Previous studies have demonstrated that relying solely on visual identification is inadequate when examining microplastics (Kroon et al., 2018; Song et al., 2015). Microplastic research that solely relies on visual identification and the absence of blank procedure tends to overestimate the presence of microplastics in the environment (Manullang et al., 2023). This study identified a slightly different type of polymer to what has been previously reported in the Pacific Ocean (Peng et al., 2018). It was found that PVEMA (43 %) and PEST (22 %) were the most common polymer identified. However, a previous study conducted in the Pacific Ocean reported a predominant PEST polymer (19 %) (Peng et al., 2018). While the Raman-Spectroscopy analysis was unable to identify the origin of the microplastics in the samples, a review of the relevant literature can help identify the source of the plastic waste. PVEMA polymer is commonly used as a detergent builder and stabilizer in medical applications, and food packaging (Demir et al., 2017; Shahbazi et al., 2014). The PEST polymer has a wide range of applications in industries such as construction, textile, automotive, medical, and electrical. Polyester is also extensively used in the production of packaging materials like bottles and other containers (Camlibel, 2018; Zughaibi and Steiner, 2021). Polypropylene accounted for 8 % in this study and is typically used for high-temperature-resistant items such as trays, funnels, pails, infant bottles, and instrument jars (Maddah, 2016). Polypropylene is also widely used in the manufacturing of drinking straws (Roy et al., 2021). The polyurethane polymer can be used in the construction of fishing net (Huang et al., 2009).

This investigation presents novel findings on the distribution of microplastics within the deep-sea water column of the ITF pathway,

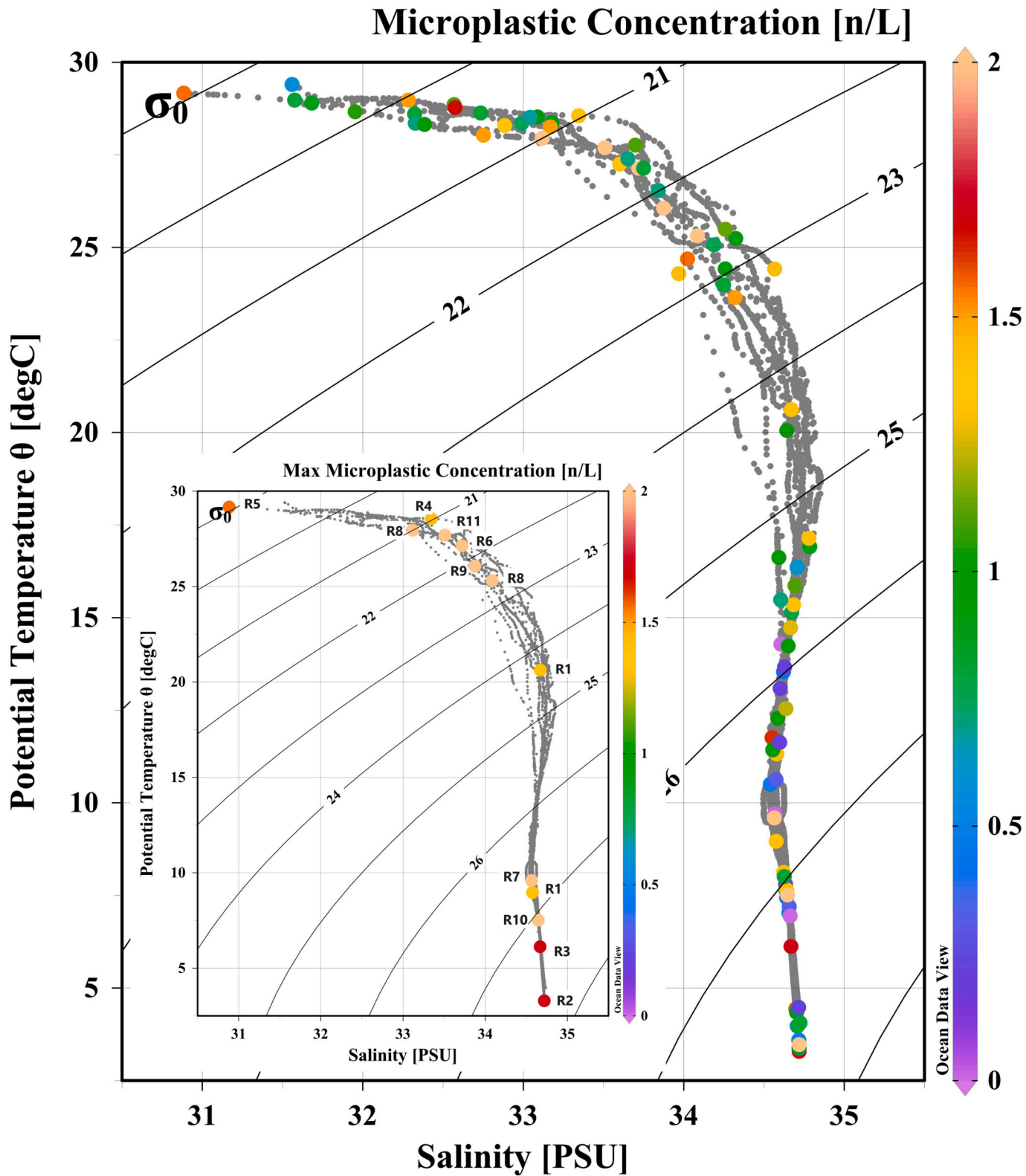


**Fig. 7.** Physical parameters (salinity, temperature and density) profile of the ITF pathway with plot microplastic abundance.

ranging from a depth of 5 m to 2450 m. The mean concentration of microplastics was  $1.062 \pm 0.646$  (0 to 3.4) n/L. The concentration of microplastics observed at the entrance of the northern Makassar Strait (R1, R2, R3) was relatively high, as depicted in Fig. 4. We hypothesized that this microplastic pollution originates from the Pacific Ocean, which flows into the Sulawesi Sea and then into the Makassar Strait. Previous

studies in the Pacific Ocean reported significant high level of microplastics (ranging from 2.06 to 13.51 n/L) (Peng et al., 2018). This assumption is supported by the observation that microplastic concentrations tend to be highest at depths between 200 m and 300 m (Fig. 6), relatively consistent with previous research indicating strong ITF currents between 100 and 400 m depth (Fan et al., 2018; Lu et al., 2023).

**Table 1**  
General Additive Model between microplastic concentration and physical parameters.

Variable predictor	p-Value
Salinity	0.607
Temperature	0.012
Density	0.047

Furthermore, it was noted that the concentration of microplastics did not increase from the entrance of Makassar Strait (R1, R2, R3) to Makassar Strait region (R4, R5, R6). Instead, there was a tendency towards a 11 % decrease. This situation may be attributed to the mechanism of microplastic deposition in the sediment. According to [Woodall et al. \(2014\)](#), certain categories of plastic materials are susceptible to losing buoyancy, leading to their eventual settling at the bottom of the ocean. The north-south section of microplastic concentration along the main gate of ITF Pathways also indicated that the basin areas seem susceptible to trapping the microplastics near the St. R5 and St. R6 ([Fig. 5](#)).

Compared to microplastic content in the entrance of Makassar Strait (R1, R2, R3), the concentration of microplastics in the St. R7 was increased 2 %. The elevated levels of microplastics observed starting from St. R7 may be attributed to the impact of microplastic accumulation originating from Pacific Ocean and as well as the local input from human activities in the surrounding area of Makassar and Kalimantan Island and input from the Java Sea. The Java Sea are one of the main ITF input paths ([Susanto et al., 2016](#)). According to the collected data, there was a marked rise in the amount of microplastics found at St. R8. The significant microplastic concentration observed at St. R8 may be attributed to the impact of microplastic accumulation originating from Pacific Ocean, the local input from human activities from Bali and Lombok. Furthermore, St. R8 is situated in close proximity to some of the most densely small islands in Indonesia, such as Bali, and Lombok ([Gaffin et al., 2004](#)). Indonesia is the second largest producer of plastic globally, with a significant portion of it accumulating in coastal areas of small islands and small to medium-sized cities ([Jambeck et al., 2015](#); [Suyadi and Manullang, 2020](#)). The microplastic concentration observed at St. R9, R10 and R11 in the Lombok Strait was comparatively lower than the average concentration recorded in the entrance of Makassar Strait (R1, R2, R3) (decreasing 10 %). This observation suggests that many microplastic particles might have been transported eastward, specifically towards the Flores and Banda Sea. Before being exported to the Indian Ocean, the Makassar Strait throughflow moves into the Flores and Banda Sea. Over a period of three decades, extensive research in this domain has consistently documented that the primary conduit for the ITF commences in the western Pacific Ocean. It then proceeds to enter the Indonesian seas by passing through the Sulawesi sills, subsequently traversing the Sulawesi Sea and the Makassar Strait. From this point, a fraction of the aqueous substance promptly departs towards the Indian Ocean through the Lombok and Alas Straits, while the predominant portion converges towards the Banda Sea and amalgamates with the eastern Indonesian Throughflow pathway prior to its departure into the Indian Ocean ([Susanto et al., 2016](#)).

The vertical transport of plastic particles in water environments can be described by various parameters, including the physical properties of seawater. The temperature, salinity, and density of water are three of the most critical physical variables ([Pawlowicz, 2013](#)). In this research study, a non-linear regression analysis using the generalized additive model (GAM) was conducted to evaluate the impact of environmental parameters (temperature, salinity, and density) on the distribution of microplastics in the ITF water column. This model was adopted to observe the relationship between the response and predictor variables without assuming linearity between the two variables. The findings of the Generalized Additive Model statistical test showed that the abundance of microplastics was significantly influenced by water

temperature and water density, while the salinity value exhibited a statistically insignificant impact. Previous research in the Atlantic Ocean has also linked water temperature parameters to the abundance of microplastic ([Lusher et al., 2014](#); [Kanhai et al., 2017](#)). The investigation by [Choy et al. \(2019\)](#) revealed the significance of density in the vertical distribution of microplastics in the epipelagic and mesopelagic zones of the California Coast. A study on the three offshore areas, including the East China Sea, Java Island in Indonesia, and Tampa Bay in the USA, demonstrated the impact of temperature on microplastic abundance by affecting the movement and density of seawater ([Liu et al., 2022](#)).

Based on the findings of this present investigation, it can be derived that the largest concentration was predominantly observed in layers other than the surface layer. These findings contribute to a practical understanding of plastic dispersion from the ocean surface, as explored in previous investigations ([Eriksen et al., 2014](#)). The latest study reported that microplastic concentration in the subsurface was 16 times higher than in the surface layer in the Antarctic seawater ([Zhang et al., 2022](#)) and 200 times higher in Eurasian Arctic ([Yakushev et al., 2021](#)). According to the data depicted in [Fig. 7](#), the maximum microplastic concentration is divided into two distinct clusters. The first cluster of stations, namely R4, R6, R8, R9, and R11, exhibited a density range ( $\sigma_t$ ) of 21–23 kg/m<sup>3</sup>. The recorded temperatures range from 25 to 28.5 °C, while the salinity levels range between 33 and 34 psu. The maximum concentration of microplastics at stations R4, R6, R8, and R9 was observed within the thermocline layer, characterized by water column stratification due to significant temperature and density changes. Meanwhile, the highest concentration value in the St. R11 was observed in the surface layer. The microplastic concentrations tabulation and thermocline graph for each station are presented in the Supplementary material, Tables S2, S3 and Figs. 2–12. It is hypothesized that the stratification of the water column due to variations in temperature and density at the thermocline layer could serve as a barrier to the sinking of microplastics. Similar findings were also documented in the Baltic Sea, where elevated levels of microplastics were observed within the stratification water column layer ([Zhou et al., 2021](#); [Uurasjärvi et al., 2020](#)).

The second cluster of stations were R1, R2, R3, R7, and R10, demonstrated in a density range ( $\sigma_t$ ) of 26–28 kg/m<sup>3</sup>, a temperature range of 3–10 °C, and a salinity range of 34–35 psu. The maximum microplastic concentrations within this group are situated in the bottom boundary layer of the thermocline layer (R1, R2) and below the thermocline layer (R3, R7, R10). It is assumed that the sinking of microplastics into deeper layers may be affected by other factors. Alongside the inherent physical characteristics of seawater, previous studies have reported various factors also influence the vertical transport of microplastics within the water column, such as turbulence ([Yang and Foroutan, 2023](#)), sedimentation and strong current ([Mancini et al., 2023](#)), biofouling ([Miao et al., 2021](#)), settling velocity of microplastic ([Francalanci et al., 2021](#)), upwelling or downwelling ([Choy et al., 2019](#)).

The determination of settling velocity has been recognized as an essential criterion for characterizing the vertical transportation of microplastics within aquatic environments ([Ballent et al., 2013](#)). However, it is important to note that the settling velocity plays a significant role in the transportation of microplastics within a calm water column ([Mancini et al., 2023](#)). The settling velocity of microplastic is determined by the density of the seawater and microplastic density as well as the shape and size of the microplastic particles ([Francalanci et al., 2021](#)). The present investigation revealed that a significant proportion of the microplastic samples analyzed consisted of fiber, accounting for 91 % of the total. Consequently, the settling velocity value in this current study was shown to be significantly impacted by the density of each type of microplastic found. The settling velocity (W) of microplastics in the ITF pathway ranges from 0.0004 to 0.0068 m/s. Plastics with low settling velocities, such as PP, were mainly found in the upper water layer at depths of 5 to 40 m. Plastics with higher settling velocities, such as PVEMA and PEST, were typically observed in deeper depths. Therefore, the high accumulation of microplastics in the deeper layers at stations

R1, R2, R3, R7, and R10 may be influenced by the relatively high settling velocity values of microplastics such as PVEMA and PEST.

Nevertheless, biofouling may also lead to transporting microplastics to deeper ocean layers (Liu et al., 2022). Choy et al. (2019) reported that the specific gravity of microplastic particles can be strongly influenced by the presence of other materials attached to them. Microplastics can experience density changes when covered with an organic or inorganic layer, causing floating microplastics to sink and sunken microplastics to slow down and remain at a certain level of depth. This phenomenon might contribute to the presence of the PPI plastic, which contains a low settling speed but was discovered in deep water layers. Similar findings were reported by Kaiser et al. (2017), wherein plastics, such as PE, characterized by low settling velocity values related to their small density, can be transferred to the bottom layer as a result of biofouling.

Despite the differences between sampling, processing, and analytical techniques for microplastic identification, the mean microplastic concentration in sub-surface waters along the ITF pathway in this study was relatively higher than that observed in the subsurface deep-sea waters across the world (the comparison of microplastic concentration between this study with other study is presented in the Supplementary material, Table S4). The microplastic content in the water column of the ITF pathway is higher than in Sumba waters (Cordova and Hernawan, 2018), North East Pacific Ocean (Desforges et al., 2014), Indian Ocean (Lusher et al., 2014), Atlantic Ocean (Courtene-Jones et al., 2017; Enders et al., 2015; Kanhai et al., 2017; Lusher et al., 2014, 2015), Artic Ocean (Kanhai et al., 2018), North Pole/Central (Ross et al., 2021), Beaufort Sea (Ross et al., 2021), Eurasian Arctic (Yakushev et al., 2021) and Antarctic seawater (Zhang et al., 2022). Whereas, the average microplastic abundance in the main of ITF was lower than that reported in the Mariana Trench (Peng et al., 2018). The higher microplastic abundances reported in this study compare to other region were possible because the sampling locations are close to the shore, which usually have higher microplastic abundances than open oceanic sites. The recent study also stated that microplastic concentration recorded in the sea surface in the Makassar Strait is higher than in the Northwestern Pacific Ocean (Yuan et al., 2023).

## 5. Conclusion

This investigation provided the first assessment of microplastic presence within the water column along the ITF pathway. The microplastic concentration values documented in this study were greater than concentration estimates for subsurface in the open ocean. The primary shape type identified in this investigation was fibers, accounting for 91 % of the total. The analysis of confirmed microplastics revealed that the predominant polymer type was PVEMA (43 %) and PEST (22 %). The statistical analysis indicated that temperature and density had a significant impact on the number of microplastics present in the water column of the ITF pathway. Our data indicate that ocean transport from the Pacific Ocean leads to the continuous accumulation of microplastics in the main ITF pathway.

## CRediT authorship contribution statement

**Corry Yanti Manullang:** Investigation, Formal analysis. **Mufti Petala Patria:** Writing – review & editing, Project administration, Funding acquisition, Conceptualization. **Agus Haryono:** Validation, Conceptualization. **Sabiqah Tuan Anuar:** Writing – review & editing, Validation, Supervision. **Muhammad Fadli:** Data curation. **Raden Dwi Susanto:** Writing – review & editing. **Zexun Wei:** Supervision.

## Declaration of competing interest

The authors declare that they have no known competing financial interests or personal relationships that could have appeared to influence the work reported in this paper.

## Data availability

Data will be made available on request.

## Acknowledgements

Sampling in the Indonesian Through Flow Pathway was funded by TRAnsport Indonesian seas, Upwelling, and Mixing Physics (TRIUMPH) joint research conducted by the Research Center for Deep Sea - Indonesian Institute of Sciences (RCDS-LIPI, now National Research and innovation Agency), the First Institute of Oceanography (FIO), and the University of Maryland. This work was also co-funded through the 2022–2023 Hibah PUTI Q2 of Universitas Indonesia (NKB656/UN2. RST/HKP.05.00/2022) and LIPI COREMAPCTI 2021–2022 (17/A/DK/2021). RDS is supported by National Aeronautics and Space Administration (NASA) grant# 80NSSC18K0777 and National Science Foundation (NSF; grant # 2242151 through the University of Maryland. We also thank Ahmad Soamole, Abdul Malik Sudin, Rafidha Dh Opier, Ary Giri Dwi Kartika, Ivan Febriansyah, Irwan Rehalat for their help in sample and data collection.

## Appendix A. Supplementary data

Supplementary data to this article can be found online at <https://doi.org/10.1016/j.marpolbul.2023.115954>.

## References

Amelinda, C., Werorilangi, S., Burhanuddin, A.I., Tahir, A., 2021. Occurrence of microplastic particles in milkfish (*Chanos chanos*) from brackishwater ponds in Bonto Manai Village, Pangkep Regency, South Sulawesi, Indonesia. IOP Conference Series: Earth and Environmental Science 763, 012058. <https://doi.org/10.1088/1755-1315/763/1/012058>.

Ayers, J.M., Strutton, P.G., Coles, V.J., Hood, R.R., Matear, R.J., 2014. Indonesian through-flow nutrient fluxes and their potential impact on Indian Ocean productivity. *Geophys. Res. Lett.* 41, 5060–5067. <https://doi.org/10.1002/2014GL060593>.

Ballent, A., Pando, S., Purser, A., Juliano, M.F., Thomsen, L., 2013. Modelled transport of benthic marine microplastic pollution in the Nazaré Canyon. *Biogeosciences* 10, 7957–7970. <https://doi.org/10.5194/bg-10-7957-2013>.

Besseling, E., Wegner, A., Foekema, E.M., Van Den Heuvel-Greve, M.J., Koelmans, A.A., 2013. Effects of microplastic on fitness and PCB bioaccumulation by the lugworm *Arenicola marina* (L.). *Environ. Sci. Technol.* 47 (1), 593–600. <https://doi.org/10.1021/es302763x>.

Bhattacharya, P., Lin, S., Turner, J.P., Ke, P.C., 2010. Physical adsorption of charged plastic nanoparticles affects algal photosynthesis. *J. Phys. Chem. C* 114, 16556–16561. <https://doi.org/10.1021/jp1054759>.

Bryden, H.L., Imaiwaki, S., 2001. Ocean transport of heat. In: Siedler, G., Church, J., Gould, J. (Eds.), *Ocean Circulation and Climate*. Academic Press, San Diego, pp. 455–475.

Camlibel, N.O. (Ed.), 2018. Polyester-Production, Characterization and Innovative Applications. InTech. <https://doi.org/10.5772/intechopen.69941>.

Choy, C.A., Robison, B.H., Gagne, T.O., Erwin, B., Firl, E., Halden, R.U., Hamilton, J.A., Katija, K., Lisin, S.E., Rolsky, C., Houtan, K.S.V., 2019. The vertical distribution and biological transport of marine microplastics across the epipelagic and mesopelagic water column. *Sci. Rep.* 9 (1), 1–9. <https://doi.org/10.1038/s41598-019-44117-2>.

Cole, M., Lindeque, P., Fileman, E., Halsband, C., Goodhead, R., Moger, J., Galloway, T. S., 2013. Microplastic ingestion by zooplankton. *Environ. Sci. Technol.* 47 (12), 6646–6655. <https://doi.org/10.1021/es400663f>.

Cordova, M.R., Hernawan, U.E., 2018. Microplastics in Sumba waters, East Nusa Tenggara. IOP Conference Series: Earth and Environmental Science 162 (1). <https://doi.org/10.1088/1755-1315/162/1/012023>.

Cordova, M.R., Purwiyanto, A.I.S., Suteja, Y., 2019. Abundance and characteristics of microplastics in the northern coastal waters of Surabaya, Indonesia. *Marine Pollution Bulletin* 142, 183–188. <https://doi.org/10.1016/j.marpolbul.2019.03.040>.

Cordova, M.R., Riani, E., Shiomoto, A., 2020. Microplastics ingestion by blue panchax fish (*Apocheilus* sp.) from Ciliwung Estuary, Jakarta, Indonesia. *Mar. Pollut. Bull.* 161, 111763 <https://doi.org/10.1016/j.marpolbul.2020.111763>.

Cordova, M.R., Ulumuddin, Y.I., Purbonegoro, T., Shiomoto, A., 2021. Characterization of microplastics in mangrove sediment of Muara Angke Wildlife Reserve, Indonesia. *Marine Pollution Bulletin* 163, 112012. <https://doi.org/10.1016/j.marpolbul.2021.112012>.

Courtene-Jones, W., Quinn, B., Gary, S.F., Mogg, A.O.M., Narayanaswamy, B.E., 2017. Microplastic pollution identified in deep-sea water and ingested by benthic invertebrates in the Rockall Trough, North Atlantic Ocean. *Environ. Pollut.* 231, 271–280. <https://doi.org/10.1016/j.envpol.2017.08.026>.

De Deckker, P., 2016. The Indo-Pacific warm pool: critical to world oceanography and world climate. *Geoscience Letters* 3, 20. <https://doi.org/10.1186/s40562-016-0054-3>.

Demir, Y.K., Metin, A.Ü., Şatiroğlu, B., Solmaz, M.E., Kayser, V., Mäder, K., 2017. Poly (methyl vinyl ether-co-maleic acid) – pectin based hydrogel-forming systems: gel, film, and microneedles. *Eur. J. Pharm. Biopharm.* 117, 182–194. <https://doi.org/10.1016/j.ejpb.2017.04.018>.

Desforges, J.W., Galbraith, M., Dangerfield, N., Ross, P.S., 2014. Widespread distribution of micoplastics in subsurface seawater in the NE Pacific Ocean. *Mar. Pollut. Bull.* 79 (1–2), 94–99. <https://doi.org/10.1016/j.marpolbul.2013.12.035>.

Enders, K., Lenz, R., Stedmon, C.A., Nielsen, T.G., 2015. Abundance, size and polymer composition of marine microplastics  $\geq 10 \mu\text{m}$  in the Atlantic Ocean and their modelled vertical distribution. *Mar. Pollut. Bull.* 100, 70–81. <https://doi.org/10.1016/j.marpolbul.2015.09.027>.

Erkisen, M., Lebreton, L.C.M., Carson, H.S., Thiel, M., Moore, C.J., Borerro, J.C., Galgani, F., Ryan, J.R., 2014. Plastic pollution in the world's oceans: more than 5 trillion plastic pieces weighing over 250,000 tons afloat at sea. *PLoS One* 9 (12), e111913. <https://doi.org/10.1371/journal.pone.0111913>.

Falahudin, D., Cordova, M.R., Sun, X., Yogaswara, D., Wulandari, I., Hindarti, D., Arifin, Z., 2020. The first occurrence, spatial distribution and characteristics of microplastic particles in sediments from Banten Bay, Indonesia. *Science of The Total Environment* 705, 135304. <https://doi.org/10.1016/j.scitotenv.2019.135304>.

Fan, W., Jian, Z., Chu, Z., Dang, H., Wang, Y., Bassinot, F., Han, X., Bian, Y., 2018. Variability of the Indonesian throughflow in the Makassar Strait over the last 30 ka. *Sci. Rep.* 8 (1), 1–8. <https://doi.org/10.1038/s41598-018-24055-1>.

Ffield, A., Gordon, A.L., 1996. Tidal mixing signatures in the Indonesian seas. *J. Phys. Oceanogr.* 26, 1924–1937. [https://doi.org/10.1175/1520-0485\(1996\)026<1924:TMSITI>2.0.CO;2](https://doi.org/10.1175/1520-0485(1996)026<1924:TMSITI>2.0.CO;2).

Francalanci, S., Paris, E., Solari, L., 2021. On the prediction of settling velocity for plastic particles of different shapes. *Environ. Pollut.* 290, 118068 <https://doi.org/10.1016/j.envpol.2021.118068>.

Gaffin, S.R., Rosenzweig, C., Xing, X., Yetman, G., 2004. Downscaling and geo-spatial gridding of socio-economic projections from the IPCC Special Report on Emissions Scenarios (SRES). *Glob. Environ. Chang.* 14 (2), 105–123. <https://doi.org/10.1016/j.gloenvcha.2004.02.004>.

Germanov, E.S., Marshall, A.D., Hendrawan, I.G., Admiraal, R., Rohner, C.A., Argeswara, J., Wulandari, R., Himawan, M.R., Loneragan, N.R., 2019. Microplastics on the menu: plastics pollute Indonesian manta ray and whale shark feeding grounds. *Front. Mar. Sci.* 6 <https://doi.org/10.3389/fmars.2019.00679>.

Gordon, A.L., Susanto, R.D., Ffield, A.L., 1999. Throughflow within Makassar Strait. *Geophys. Res. Lett.* 26 (21), 3325–3328. <https://doi.org/10.1029/1999GL002340>.

Gordon, A.L., Susanto, R.D., Ffield, A., Huber, B., Pranowo, W., Wirasantosa, S., 2008. Makassar Strait Throughflow 2004–2006. *Geophys. Res. Lett.* 35, L24605 <https://doi.org/10.1029/2008GL036372>.

Gorgues, T., Menkes, C., Autmont, O., Dandonneau, Y., Madec, G., Rodgers, K., 2007. Indonesian throughflow control of the eastern equatorial Pacific biogeochemistry. *Geophys. Res. Lett.* 34, 5. <https://doi.org/10.1029/2006GL028210>.

Hayatama, T., 2004. Transformation of the Indonesian throughflow water by vertical mixing and its relation to tidally generated internal waves. *J. Oceanogr.* 60 (3), 569–585. <https://doi.org/10.1023/B:JOCE.0000038350.32155.cb>.

Hautala, S.L., Reid, J.L., Bray, N., 1996. The distribution and mixing of Pacific water masses in the Indonesian Seas. *J. Geophys. Res. Oceans* 101 (C5), 12375–12389. <https://doi.org/10.1029/96JC00037>.

Horton, A.A., Walton, A., Spurgeon, D.J., Lahive, E., Svendsen, C., 2017. Microplastics in freshwater and terrestrial environments: evaluating the current understanding to identify the knowledge gaps and future research priorities. *Sci. Total Environ.* 586, 127–141. <https://doi.org/10.1016/j.scitotenv.2017.01.190>.

Huang, Jere-Yue, Lin, Wei-Ting, Huang, Ran, Lin, Chih-Yang, Wu, Jiann-Kuo, 2009. Marine biofouling inhibition by polyurethane conductive coatings used for fishing net. *Journal of Coatings Technology Research* 7, 111–117. <https://doi.org/10.1007/s11998-008-9151-3>.

Isyirini, R., Nafie, Y.A.L., Ukkas, M., Rachim, R., Cordova, M.R., 2019. Marine macro debris from Makassar Strait beaches with three different designations. *IOP Conference Series: Earth and Environmental Science* 253 (1). <https://doi.org/10.1088/1755-1315/253/1/012039>.

Jambeck, J.R., Geyer, R., Wilcox, C., Siegler, T.R., Perryman, M., Andrade, A., Narayan, R., Law, K.L., 2015. Plastic waste inputs from land into the ocean. *Science* 347, 768–771. <https://doi.org/10.1126/science.1260352>.

Kaiser, D., Kowalski, N., Waniek, J.J., 2017. Effects of biofouling on the sinking behavior of microplastics. *Environ. Res. Lett.* 12 (12) <https://doi.org/10.1088/1748-9326/aa8e8b>.

Kama, N.A., Rahim, S.W., Yaqin, K., 2021. Microplastic concentration in column seawater compartment in Berau, Luwu Regency, South Sulawesi, Indonesia. *IOP Conference Series: Earth and Environmental Science* 763 (1). <https://doi.org/10.1088/1755-1315/763/1/012061>.

Kanhai, L.D.K., Officer, R., Lyashevskaya, O., Thompson, R.C., O'Connor, I., 2017. Microplastic abundance, distribution and composition along a latitudinal gradient in the Atlantic Ocean. *Mar. Pollut. Bull.* 115 (1–2), 307–314. <https://doi.org/10.1016/j.marpolbul.2016.12.025>.

Kanhai, L.D.K., Gårdfeldt, K., Lyshevskaya, O., Hassellöv, M., Thompson, R.C., O'Connor, I., 2018. Microplastics in sub-surface waters of the Arctic Central Basin. *Mar. Pollut. Bull.* 130, 8–18. <https://doi.org/10.1016/j.marpolbul.2016.12.025>.

Koch-Larrouy, A., Madec, G., Bourret-Aubertot, P., Gerkema, T., Bessières, L., Molcard, R., 2007. On the transformation of Pacific Water into Indonesian Throughflow Water by internal tidal mixing. *Geophys. Res. Lett.* 34 (L04), 604. <https://doi.org/10.1029/2006GL028405>.

Kroon, F., Motti, C., Talbot, S., Sobral, P., Puotinen, M., 2018. A workflow for improving estimates of microplastic contamination in marine waters: a case study from North-Western Australia. *Environ. Pollut.* 238, 26–38. <https://doi.org/10.1016/j.envpol.2018.03.010>.

Lee, T., Fukumori, I., Menemenlis, D., Xing, Z., Fu, L.-L., 2002. Effects of the Indonesian throughflow on the Pacific and Indian Ocean. *J. Phys. Oceanogr.* 32, 1404–1429.

Lee, K.W., Shim, W.J., Kwon, O.Y., Kang, J.H., 2013. Size-dependent effects of micro polystyrene particles on the marine copepod *Tigriopus japonicus*. *Environ. Sci. Technol.* 47, 11278–11283. <https://doi.org/10.1021/es401932b>.

Lee, S.-K., Park, W., Baringer, M.O., Gordon, A.L., Huber, B., Liu, Y., 2015. Pacific origin of the abrupt increase in Indian Ocean heat content during the warming hiatus. *Nat. Geosci.* 8 (6), 445–449. <https://doi.org/10.1038/ngeo2438>.

Lee, T., Fournier, S., Gordon, A.L., Sprintall, J., 2019. Maritime continent water cycle regulates low-latitude chokepoint of global ocean circulation. *Nature Communications* 10 (1), 2103. <https://doi.org/10.1038/s41467-019-10109-z>.

Liu, J., Liu, H., He, D., Zhang, T., Qu, J., Lv, Y., Zhang, Y., 2022. Comprehensive effects of temperature, salinity, and current velocity on the microplastic abundance in offshore area. *Pol. J. Environ. Stud.* 31 (2), 1727–1736. <https://doi.org/10.15244/pjoes/142389>.

Lu, X., Hu, S., Guan, C., Li, M., Sprintall, J., Wang, F., 2023. Quantifying the contribution of salinity effect to the seasonal variability of the Makassar Strait throughflow. *Geophys. Res. Lett.* 50, e2023GL105991 <https://doi.org/10.1029/2023GL105991>.

Lusher, A.L., Burke, A., O'Connor, I., Officer, R., 2014. Microplastic pollution in the Northeast Atlantic Ocean: validated and opportunistic sampling. *Mar. Pollut. Bull.* 88, 325–333. <https://doi.org/10.1016/j.marpolbul.2014.08.023>.

Lusher, A.L., Tirelli, V., O'Connor, I., Officer, R., 2015. Microplastics in Arctic polar waters: the first reported values of particles in surface and sub-surface samples. *Sci. Rep.* 5, 1–10. <https://doi.org/10.1038/srep14947>.

Maddah, H., 2016. Polypropylene as a promising plastic: a review. *American Journal of Polymer Science* 2016 6 (1), 1–11. <https://doi.org/10.5923/j.ajps.20160601.01>.

Makarim, S., Sprintall, J., Liu, Z., Yu, W., Santoso, A., Yan, X.-H., Susanto, R.D., 2019. Previously unidentified Indonesian Throughflow pathways and freshening in the Indian Ocean during recent decades. *Sci. Rep.* 9, 7364. <https://doi.org/10.1038/s41598-019-43841-z>.

Mancini, M., Serra, T., Colomer, J., Solari, L., 2023. Suspended sediments mediate microplastic sedimentation in unidirectional flows. *Sci. Total Environ.* 890, 164363 <https://doi.org/10.1016/j.scitotenv.2023.164363>.

Manullang, C.Y., Patria, M.P., Haryono, A., Anuar, S.T., Suyadi, Opier, R.D.A., 2023. Status and research gaps of microplastics pollution in Indonesian waters: a review. *Indonesian Journal of Chemistry* 23 (1), 251–267. <https://doi.org/10.22146/jic.73485>.

Metzger, E.J., Hurlburt, H.E., Xu, X., Shriner, J.F., Gordon, A.L., Sprintall, J., Susanto, R.D., van Aken, H.M., 2010. Simulated and observed circulation in the Indonesian seas: 1/12° global HYCOM and the INSTANT observations. *Dynamics of Atmospheres and Oceans* 50, 275–300. <https://doi.org/10.1016/j.dynatmoce.2010.04.002>.

Miao, L., Gao, Y., Adyel, T.M., Huo, Z., Liu, Z., Wu, J., Hou, J., 2021. Effects of biofilm colonization on the sinking of microplastics in three freshwater environments. *J. Hazard. Mater.* 413, 125370 <https://doi.org/10.1016/j.jhazmat.2021.125370>.

Nagai, T., Hibiya, T., 2015. Internal tides and associated vertical mixing in the Indonesian Archipelago. *J. Geophys. Res.* 120, 3373–3390. <https://doi.org/10.1002/2014JC010592>.

Nagai, T., Hibiya, T., Syamsudin, F., 2021. Direct estimates of turbulent mixing in the Indonesian archipelago and its role in the transformation of the Indonesian throughflow waters. *Geophys. Res. Lett.* 48 (6) <https://doi.org/10.1029/2020GL091731>.

Napper, I.E., Thompson, R.C., 2016. Release of synthetic microplastic plastic fibres from domestic washing machines: effects of fabric type and washing conditions. *Mar. Pollut. Bull.* 112 (12), 39–45. <https://doi.org/10.1016/j.marpolbul.2016.09.025>.

Ningrum, E.W., Patria, M.P., 2022. Microplastic contamination in Indonesian anchovies from fourteen locations. *Biodiversitas* 23 (1), 125–134. <https://doi.org/10.13057/biodiv/d230116>.

Obbard, R.W., Sadri, S., Wong, Y.Q., Khitun, A.A., Baker, I., Thompson, R.C., 2014. Global warming releases microplastic legacy frozen in Arctic Sea ice. *Earth's Future* 2 (6), 315–320. <https://doi.org/10.1002/2014EF000240>.

Pawlowicz, R., 2013. Key physical variables in the ocean: temperature, salinity, and density. *Nature Education Knowledge* 4 (4), 13.

Peng, X., Chen, M., Chen, S., Dasgupta, S., Xu, H., Ta, K., Du, M., Li, J., Guo, Z., Bai, S., 2018. Microplastics contaminate the deepest part of the world's ocean. *Geochemical Perspectives Letters* 9, 1–5. <https://doi.org/10.7185/geochemlet.1829>.

Ray, R.D., Susanto, R.D., 2016. Tidal mixing signatures in the Indonesian seas from high-resolution sea-surface temperature. *Geophys. Res. Lett.* 43 (15) <https://doi.org/10.1002/2016GL069485>.

Ray, R.D., Susanto, R.D., 2019. A fortnightly atmospheric 'tide' at Bali caused by oceanic tidal mixing in Lombok Strait. *Geosciences Letters* 6 (6), 1–9. <https://doi.org/10.1186/s40562-019-0135-1>.

Rochman, C.M., Tahir, A., Williams, S.L., Baxa, D.V., Lam, R., Miller, J.T., The, F.C., Werorilangi, S., The, S.J., 2015. Anthropogenic debris in seafood: plastic debris and fibers from textiles in fish and bivalves sold for human consumption. *Sci. Rep.* 5, 1–10.

Ross, P.S., Chastain, S., Vassilenko, E., Etemadifar, A., Zimmermann, S., Quesnel, S., Eert, J., Solomon, E., Patankar, S., Posacka, A.M., Williams, B., 2021. Pervasive distribution of polyester fibres in the Arctic Ocean is driven by Atlantic inputs. *Nat. Commun.* 12 (1), 1–9. <https://doi.org/10.1038/s41467-020-20347-1>.

Roy, P., Ashton, L., Wang, T., Corradini, M.G., Fraser, E.D., Thimmanagari, M., Tiessan, M., Bali, A., Saharan, K.M., Mohanty, A.K., Misra, M., 2021. Evolution of

drinking straws and their environmental, economic and societal implications. *J. Clean. Prod.* 316, 128234. <https://doi.org/10.1016/j.jclepro.2021.128234>.

Sawalman, R., Putri Zamani, N., Werorilangi, S., Samira Ismet, M., 2021. Spatial and temporal distribution of microplastics in the surface waters of Barranglomo Island, Makassar. *IOP Conference Series: Earth and Environmental Science* 860 (1). <https://doi.org/10.1088/1755-1315/860/1/012098>.

Shahbazi, A., Almeida, P.V., Mäkilä, E., Correia, A., Ferreira, M.P., Kaasalainen, M., Salonen, J., Hirvonen, J., Santos, H.A., 2014. Poly(methyl vinyl ether-alt-maleic acid)-functionalized porous silicon nanoparticles for enhanced stability and cellular internalization. *Macromol. Rapid Commun.* 35 (6), 624–629. <https://doi.org/10.1002/marc.201300868>.

Shinoda, T., Han, W., Metzger, E.J., Hurlburt, H., 2012. Seasonal variation of the Indonesian throughflow in Makassar Strait. *J. Phys. Oceanogr.* 42, 1099–1123. <https://doi.org/10.1175/JPO-D-11-0120.1>.

Shinoda, T., Han, W., Jensen, T.G., Zamudio, L., Metzger, E.J., Lien, R.-C., 2016. Impact of the Madden-Julian Oscillation on the Indonesian Throughflow in Makassar Strait during the CINDY/DYNAMO field campaign. *J. Climate* 29 (17), 6085–6108. <https://doi.org/10.1175/JCLI-D-15-0711.1>.

Song, Y.K., Hong, S.H., Jang, M., Han, G.M., Rani, M., Lee, J., Shim, W.J., 2015. A comparison of microscopic and spectroscopic identification methods for analysis of microplastics in environmental samples. *Mar. Pollut. Bull.* 93 (1–2), 202–209. <https://doi.org/10.1016/j.marpolbul.2015.01.015>.

Sprintall, J., Wijffels, S.E., Mocard, R., Jaya, I., 2009. Direct estimates of the Indonesian throughflow entering the Indian Ocean: 2004–2006. *J. Geophys. Res.* 114, C07001. <https://doi.org/10.1029/2008JC005257>.

Sprintall, J., Gordon, A.L., Koch-Larrouy, A., Lee, T., Potemra, J.T., Pujiana, K., Wijffels, S.E., 2014. The Indonesian seas and their role in the coupled ocean-climate system. *Nature Geoscience* 7, 487–492. <https://doi.org/10.1038/ngeo2188>.

Sprintall, J., Gordon, A.L., Wijffels, S.E., Feng, M., Hu, S., Koch-Larrouy, A., Phillips, H., Nugroho, D., Napitu, A., Pujiana, K., Susanto, R.D., Sloyan, B., Peña-Molino, B., Yuan, D., Riaima, N.F., Siswanto, S., Kuswardani, A., Arifin, Z., Wahyudi, A.J., Zhou, H., Nagai, T., Ansong, J.K., Bourdalle-Badié, R., Chanut, J., Lyard, F., Arbic, B. K., Ramdhani, A., Setiawan, A., 2019. Detecting change in the Indonesian seas. *Front. Mar. Sci.* 6, 257. <https://doi.org/10.3389/fmars.2019.00257>.

Susanto, R.D., Gordon, A.L., 2005. Velocity and transport of Indonesian throughflow in Makassar Strait. *J. Geophys. Res.* 110, C01005. <https://doi.org/10.1029/2004JC002425>.

Susanto, R.D., Ray, R.D., 2022. Seasonal and interannual variability of tidal mixing signatures in Indonesian seas from high-resolution sea surface temperature. *Remote Sens. (Basel)* 14, 1934. <https://doi.org/10.3390/rs14081934>.

Susanto, R.D., Gordon, A.L., Sprintall, J., Herunadi, B., 2000. Intraseasonal variability and tides in Makassar Strait. *Geophys. Res. Lett.* 27, 1499–1502. <https://doi.org/10.1029/2000GL011414>.

Susanto, R.D., Field, A., Gordon, A.L., Adi, T.R., 2012. Variability of Indonesian throughflow with Makassar Strait: 2004–2009. *J. Geophys. Res.* 117, C09013. <https://doi.org/10.1029/2012JC008096>.

Susanto, R.D., Wei, Z., Adi, T.R., Zheng, Q., Fang, G., Fan, B., Supangat, A., Agustiadi, T., Li, S., Trenggono, M., Setiawan, A., 2016. Oceanography surrounding Krakatau volcano in the Sunda Strait, Indonesia. *Oceanography* 29 (2), 228–237. <https://doi.org/10.5670/oceanog.2016.31>.

Sussarellu, R., Suquet, M., Thomas, Y., Lambert, C., Fabioux, C., Pernet, M.E.J., Goïc, N. L., Quillien, V., Mingant, C., Epelboin, Y., Corporeau, C., Guyomrhc, J.G., Robbins, J.R., Paul-Pont, I., Soudant, P., Huvel, A., 2016. Oyster reproduction is affected by exposure to polystyrene microplastics. *Proc. Natl. Acad. Sci.* 113 (9), 2430–2435. <https://doi.org/10.1073/pnas.1519019113>.

Suteja, Y., Atmadipoera, A.S., Riani, E., Nurjaya, I.W., Nugroho, D., Cordova, M.R., 2021. Spatial and temporal distribution of microplastic in surface water of tropical estuary: case study in Benoa Bay, Bali, Indonesia. *Marine Pollution Bulletin* 163, 111979. <https://doi.org/10.1016/j.marpolbul.2021.111979>.

Suyadi, Manullang, C.Y., 2020. Distribution of plastic debris pollution and its implications on mangrove vegetation. *Marine Pollution Bulletin* 160, 111642. <https://doi.org/10.1016/j.marpolbul.2020.111642>.

Tahir, A., Samawi, M.F., Sari, K., Hidayat, R., Nimzet, R., Wicaksono, E.A., Asrul, L., Werorilangi, S., 2019a. Studies on microplastic contamination in seagrass beds at Spermonde Archipelago of Makassar Strait, Indonesia. *Journal of Physics: Conference Series* 1341 (2), 022008. <https://doi.org/10.1088/1742-6596/1341/2/022008>.

Tahir, A., Taba, P., Samawi, M.F., Werorilangi, S., 2019b. Microplastics in water, sediment and salts from traditional salt producing ponds. *Global Journal of Environmental Science and Management* 5 (4), 431–440. <https://doi.org/10.22034/GJESM.2019.04.03>.

Tahir, A., Soeprarto, D.A., Sari, K., Wicaksono, E.A., Werorilangi, S., 2020. Microplastic assessment in seagrass ecosystem at Kodingareng Lombo Island of Makassar City. *IOP Conference Series: Earth and Environmental Science* 564, 012032. <https://iopscience.iop.org/article/10.1088/1755-1315/564/1/012032>.

Uurasjärvi, E., Pääkkönen, M., Setälä, O., Koistinen, A., Lehtiniemi, M., 2020. Microplastics accumulate to thin layers in the stratified Baltic Sea. *Environ. Pollut.* 268, 115700. <https://doi.org/10.1016/j.envpol.2020.115700>.

Van Cauwenbergh, L., Vanreusel, A., Mees, J., Janssen, C.R., 2013. Microplastic pollution in deep-sea sediments. *Environ. Pollut.* 182, 495–499. <https://doi.org/10.1016/j.envpol.2013.08.013>.

Vassilenko, K., Watkins, M., Chastain, S., Posacka, A., Ross, P., 2019. Me, my clothes and the ocean: the role of textiles in microfiber pollution. In: *Ocean Wise Conservation Association Science Feature*, Vancouver Canada (15 pp.).

Von Moos, N., Burkhardt-Holm, P., Köhler, A., 2012. Uptake and effects of microplastics on cells and tissue of the blue mussel *Mytilus edulis* L. after an experimental exposure. *Environmental Science & Technology* 46 (20), 11327–11335. <https://doi.org/10.1021/es302332w>.

Wang, S., Chen, H., Zhou, X., Tian, Y., Lin, C., Wang, W., Zhou, K., Zhang, Y., Lin, H., 2020. Microplastic abundance, distribution and composition in the mid-west Pacific Ocean. *Environmental Pollution* 264, 114125. <https://doi.org/10.1016/j.envpol.2020.114125>.

Wicaksono, E.A., Tahir, A., Werorilangi, S., 2020. Preliminary study on microplastic pollution in surface-water at Tallo and Jeneberang Estuary, Makassar, Indonesia. *AACL Bioflux* 13 (2), 902–909.

Woodall, L.C., Sanchez-Vidal, A., Canals, M., Paterson, G.L.J., Coppock, R., Sleight, V., Calafat, A., Rogers, A.D., Narayanaswamy, B.E., Thompson, R.C., 2014. The deep sea is a major sink for microplastic debris. *Royal Society Open Science* 1 (4). <https://doi.org/10.1098/rsos.140317>.

Yakushev, E., Gebruk, A., Osadchiev, A., Pakhomova, S., Lusher, A., Berezina, A., van Bavel, B., Vorozheikina, E., Chernykh, D., Kolbasova, G., Razgon, I., Semiletov, I., 2021. Microplastics distribution in the Eurasian Arctic is affected by Atlantic waters and Siberian rivers. *Communications Earth & Environment* 2, 1–11. <https://doi.org/10.1038/s43247-021-00091-0>.

Yang, H., Foroutan, H., 2023. Effects of near-bed turbulence on microplastics fate and transport in streams. *Sci. Total Environ.* 905, 167173. <https://doi.org/10.1016/j.scitotenv.2023.167173>.

Yuan, D., Corvianawati, C., Cordova, M.R., Surinati, D., Li, Y., Wang, Z., Li, X., Li, R., Wang, J., He, L., Yuan, A.N., Dirhamsyah, D., Arifin, Z., Sun, X., Isobe, A., 2023. Microplastics in the tropical Northwestern Pacific Ocean and the Indonesian seas. *J. Sea Res.* 194 (10240), 6. <https://doi.org/10.1016/j.seares.2023.102406>.

Zhang, S., Zhang, W., Ju, M., Qu, L., Chu, X., Huo, C., Wang, J., 2022. Distribution characteristics of microplastics in surface and subsurface Antarctic seawater. *Sci. Total Environ.* 838, 156051. <https://doi.org/10.1016/j.scitotenv.2022.156051>.

Zhao, S., Zhu, L., Wang, T., Li, D., 2014. Suspended microplastics in the surface water of the Yangtze Estuary System, China: first observations on occurrence, distribution. *Mar. Pollut. Bull.* 86, 562–568. <https://doi.org/10.1016/j.marpolbul.2014.06.032>.

Zhou, Q., Tu, C., Yang, J., Fu, C., Li, Y., Wanek, J.J., 2021. Trapping of microplastics in halocline and turbidity layers of the semi-enclosed Baltic Sea. *Front. Mar. Sci.* 8, 761566. <https://doi.org/10.3389/fmars.2021.761566>.

Zughaibi, T.A., Steiner, R.R., 2021. Forensic analysis of polymeric carpet fibers using direct analysis in real time coupled to an AccuTOFT mass spectrometer. *Polymers* 13 (16), 2687. <https://doi.org/10.3390/polym13162687>.